MARTENSITIC PHASE TRANSFORMATION IN SHAPE-MEMORY ALLOYS

by

A. A. Golestaneh

Prepared for

International Conference

on

Martensitic Transformation

Cambridge, Massachusetts

June 24, 1979

ARGONNE NATIONAL LABORATORY, ARGONNE, ILLINOIS

Operated under Contract W-31-109-Eng-38 for the

U. S. DEPARTMENT OF ENERGY

Martensitic Phase Transformation in Shape-memory Alloys

A. A. Golestaneh

This paper describes isothermal studies of the shape-recovery phenomenon, stress-strain behavior, electrical resistivity and thermoelectric power associated with the martensite-parent phase reaction in the Ni-Ti shape-memory alloys. The energy-balance equation that links the reaction kinetics with the strain energy change during the "cooling-deforming and heating" cycle is analyzed. The strain range in which the Clausius-Clapeyron equation satisfactorily describes this reaction is determined. A large change in the Young's modulus of the specimen is found to be associated with the M→P reaction. A hysteresis loop in the resistivity-temperature plot is found and related to the anomaly in the athermal resistivity changes during cyclic M→P→M transformation. An explanation for the resistivity anomaly is offered. The M structure is found to be electrically negative relative to the P structure. A thermal emf of $\gtrsim$0.12 mV is found at the M-P interface.

I. Introduction

The purpose of the present paper is to report on several features of martensitic transformation in Nitinol alloys [1], a subgroup of the shape-memory (SM) alloys. The overall objective is to correlate the kinetics of this reaction with the parameters that characterize the material structure and with the thermodynamic parameters temperature, stress, and strain (T, σ and ε). The martensitic transformation is known to exhibit a marked sensitivity to internal stresses and, at least for Nitinol alloys, to material composition [2]. Also, the heat-transfer coefficient between the specimen and the cold reservoir (CR) or hot reservoir (HR) affects the kinetics of the shape-recovery phenomenon (SRP). To analyze these effects we have performed isothermal and isobaric experiments involving (T, σ, ε) and time t. The cooling and heating medium is water, or water plus some antifreeze substance for T either below 0°C or above 100°C. The phenomena under study are the SRP, variation of Young's modulus and electrical resistivity, and generation of thermoelectric power. Because of the technological interest in Nitinol and because of some anomalies observed in the martensite (M)-parent (P) phase reaction in these alloys, our initial studies have utilized a Ti-Ni binary alloy of 50-50 composition. The generalization of our results requires study of other binary and ternary Nitinol alloys as well as other SM materials. Because single-crystal Nitinol specimens are difficult to prepare and too expensive for practical applications, we have used polycrystalline specimens. The best isothermal test results are obtained with a wire specimen of 0.5 to

---

Materials Science Division, Argonne National Laboratory, Argonne, IL 60439, USA.

1 mm dia. The specimens are trained to have a particular form (either straight or curved with a desired radius). Inasmuch as the accurate chemical analysis of Nitinol is difficult and expensive, we characterize our specimens in terms of the M↦P transition temperature T_o, the SR critical temperature T_C, and the temperature spreads $\pm\Delta T_o$ and $\pm\Delta T_C$, which will be defined below.

For discussion of the experimental data we use the following notations. The quench-induced martensite under zero external stress will be called γ_1', while the stress-induced martensite will be called β_1'. The P phase will be designated β_1. Since our specimens are in ordered states and we are considering only reactions in which the ordering is conserved, we will henceforth omit the subscript 1. We will refer to the martensitic transformation as the M↦P or P↦M reaction.

II. The Thermomechanical Energy Equation Associated with Martensitic Transformation

We recall that shape recovery (SR) in the SM alloys is energetic and is accompanied by forces which depend on the specimen geometry and the resistance encountered. Since the magnitude and direction of the SR force are difficult to evaluate directly, we will consider the energy-balance equation that governs the SRP. The SRP is associated with the β' martensite structure, and the energy source for this phenomenon is the latent heat of the $\beta' \rightarrow \beta$ transformation $\Delta H_{\beta'\beta}$ (henceforth ΔH). For a closed martensitic transformation M↦P↦M (which does not change the geometrical or structural configuration of the specimen), the Gibbs free-energy evaluation yields the energy-balance equation [3, 4]

$$\alpha\delta\Delta H = W_o(T_H) - W_i(T_L) \quad . \tag{1}$$

Here δ is the material density, W_i is the energy required for specimen deformation at temperature $T_L < T_C$, W_o is the mechanical energy recovered in the $\beta' \rightarrow \beta$ transformation at temperature $T_H > T_C$, and α is a coefficient which relates the energy of the SR to the fraction of the M↦P transformation completed. In an energetic SR, α represents the portion of the γ' martensite which transforms via the channel

$$\gamma' \rightarrow \beta' \rightarrow \beta \tag{2}$$

and not the direct $\gamma' \rightarrow \beta$ channel [3, 4]. Reaction (2) can occur, by the so-called "reshuffling" process, because of the instability (soft mode) of the γ' martensite under the combined influence of temperature and applied stress. The coefficient α, which is always less than unity and on the order of 0.15 for binary Nitinol alloys [4], is a function of material structural parameters in addition to temperature and initial material strain, ε, and applied stress.

To evaluate α we have conducted a series of isothermal experiments. Figure 1 shows a series of isothermal stress-strain (σ-ε) tests conducted at temperatures from 20 to 105°C, a range which encompasses

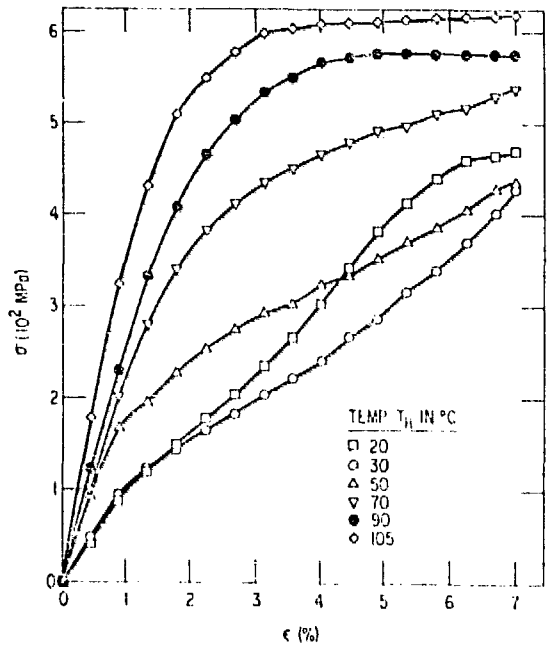

Fig. 1. Isothermally obtained stress-strain (σ-ε) curves for a Nitinol wire specimen (1 mm dia x 56 mm) with $T_C \approx 33 \pm 7°C$.

the T_C ($\approx 40°C$) of our specimen. Figure 2 shows the results of transient tests in which the specimen is strained to a certain level and its temperature is then rapidly increased from T_L to T_H. A quantity of interest is

$$\Sigma = \sigma_r(T_H) - \sigma_i(T_L) \ , \tag{3}$$

where σ_r and σ_i are, respectively, the recovery and initial stresses in the specimen. This Σ, which can be obtained from the transient curves in Fig. 2, is close to the stress difference measured in isothermal σ-ε tests (shown in Fig. 1). From the variation of the Σ value versus ε shown in Fig. 3, it is seen that for ε within the range 1.5-3.5% in our specimen, one may write

$$W_o - W_i = \frac{1}{2}\,\varepsilon_o^2\,\Delta E(T_H, T_L) + \Sigma\varepsilon \approx \Sigma\varepsilon \ . \tag{4}$$

Here ΔE is the change in the Young's modulus of the specimen due to the M$\rightarrow$P transition, and ε_o is the elastic strain limit in the specimen. By combining Eqs. (1) and (3), we obtain

$$\Sigma\varepsilon \approx \alpha\delta\Delta H \ . \tag{5}$$

The form of this equation is identical to the integrated Clausius-Clapeyron (CC) equation [5]

$$\Sigma\varepsilon = \delta\Delta H \ln\left(\frac{T_H}{T_C}\right) \qquad \text{for } T_H \lesssim A_f \ , \tag{6}$$

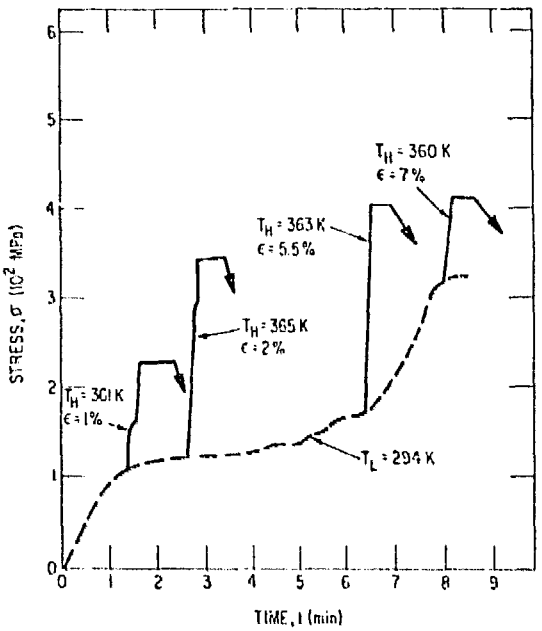

Fig. 2. Transient (σ-ε) response of a Nitinol wire specimen subjected to rapid temperature changes.

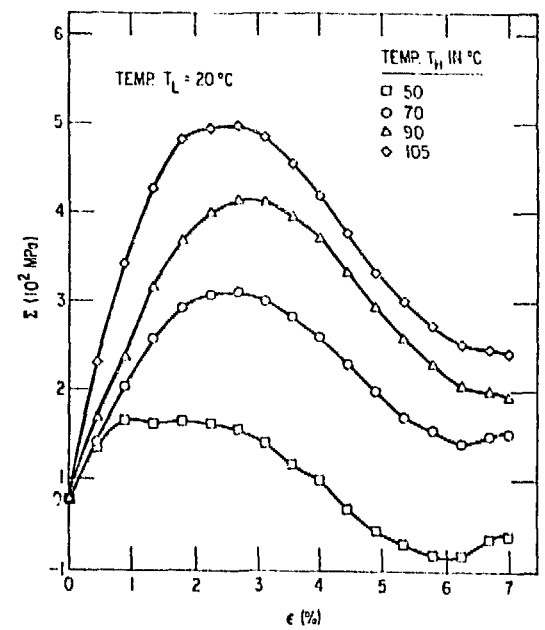

Fig. 3. Variation of $\Sigma = \sigma_r(T_H) - \sigma_i(T_L)$ with strain ε at various temperatures.

Using the data of Fig. 3, we have verified that in the range $1.5\% < \varepsilon < 3.5\%$, and for $T_L \gtrsim 0$ to 20°C, the Σ data vary fairly linearly with $\ln T_H/T_C$. The slope of this line gives, according to Eq. (6), $\Delta H = 1.2\text{-}2.8$ cal/g ($\delta = 6.3$ g/cm^3 for Nitinol alloys), which is close to $\Delta H = 1.57\text{-}2.4$ cal/g obtained previously by calorimetry [6]. This result indicates the ε range in which the CC [7] equation can be used satisfactorily. In this range Eqs. (1) and (6) give the maximum value of α, as

$$\alpha_o = \ln\left(\frac{T_H}{T_C}\right) \qquad \text{for } 1.5\% < \varepsilon < 3.5\%,\ T_H \lesssim A_f \ . \tag{7}$$

For our Nitinol alloy specimen, which has $T_C \gtrsim 313$ K and $T_H = 360$ K, Eq. (7) gives $\alpha_o = 0.140$.

To summarize the above results, (a) the CC equation is applicable in the strain range that corresponds to the bulk of the M>P transition, and (b) the coefficient α in the energy-balance equation for the above ε range depends logarithmically on T_H and T_C. It should be noted that the energetic SR depends on α and ε. However, the experimental data on the SR strain ε_r in a uniaxial system fit the expression

$$\varepsilon_r = \varepsilon_i \left\{1 - \left[\exp -\left(\frac{t}{\tau}\right)^{1/2}\right]\right\} \tag{8}$$

where ε_i is the maximum shape recovery and τ is a time constant, dependent on T_H, T_C, and ΔT_C, which arises as the result of structural inhomogeneity, the external stresses exerted on the specimen, and the heat transfer rate between the specimen and its heating medium. The factor τ is a measure of the internal friction in the specimen; thus it depends on the material structural parameters. For our annealed specimen undergoing a free SR in water, τ is about 10^{-1} sec for T_H between A_s and A_f, and it becomes much larger in the presence of a constraint stress that exceeds the σ value for a given T_H (shown in Fig. 1).

To see the effect of the grain size on α_o, we reevaluate the energy-balance equation (1) for a given grain within the specimen. For this we recall one of the conditions for the occurrence of a complete SR in an SM element, which is the conservation of the mass of the individual grains during the cooling-deformation and heating of the specimen. Thus at the onset of the SR of a grain with, say, γ' structure, volume v, and surface area s, we have

$$v\Delta W_v - s\Delta W_s = 0 \ . \tag{9}$$

Here ΔW_v and ΔW_s are, respectively, the averaged volume and surface energy densities of the grain, which appear as a result of the grain, which appear as a result of the heating of the specimen to temperature T_H. In a specimen for which a uniaxial stress is dominant

(e.g., a long, thin wire), we have $\Delta W_v = \Sigma c$, and $\Delta W_s \propto \Sigma c$. Thus, assuming all grains in the specimen have more or less the same size and are uniformly distributed, Eqs. (6) and (9) give

$$T_\sigma = T_C \left[1 + \frac{4N^{1/2}}{\delta d} \frac{\Delta W_s}{\Delta H} \right]. \tag{10}$$

Here $T_\sigma = T_H$ is the SR critical temperature corresponding to a given set of Σ and ε values, d is the average diameter of the specimen cross section, and N is the average number of grains in the cross section. Equation (10) shows that T_σ increases with d^{-1} (as reported in Ref. 8 and seen in Fig. 5 below) and with $N^{1/2}$.

III. The SRP and Other Features of the Martensitic Transformation

It is understood that the direct $\gamma' \rightarrow \beta$ transition does not directly contribute to the SRP, and that the $\beta' \rightarrow \beta$ transformation does not coincide with the SR behavior with respect to time or temperature. It is reasonable to assume that the M$\rightarrow$P reaction begins earlier than the SR, since the reaction must overcome the internal friction and stresses before the SR can start. Isothermal tests show that in the existing SM alloys under zero stress, there is a temperature T_C^- below which no SR occurs, and a temperature T_C^+ above which a complete SR occurs; the spread, $\pm\Delta T_C$, of T_C is defined by the expression $2\Delta T_C = T_C^+ - T_C^-$. One would expect $T_C^- \geq M_s$ and $T_C^+ \geq A_s$, but T_C cannot be evaluated in terms of the usual M and A temperatures, which are not themselves well defined and measurable. Rather, T_C may be determined for a thin wire by carefully deforming the specimen to a certain degree (at a temperature at which no SR can occur), quenching it in an HR at a constant temperature, and measuring the fraction of the SR. The test results in Fig. 4 show that T_C and ΔT_C depend on the specimen size and structure, with ΔT_C ranging from $\sim$7 to 15°C.

To relate the temperature T_C to the M$\rightarrow$P transition temperature T_o, we have studied other isothermal phenomena. The investigation of those features that are associated with the $\gamma' \rightleftarrows \beta$ reactions under zero stress is reported in the present work. The effect of the applied stress, which elicits the $\beta' \rightleftarrows \beta$ reactions, will be presented in a separate article.

(a) Study of the Young's modulus of the material. One of the striking observations in the pattern of the σ-ε curves describing the M$\rightarrow$P reaction is the substantial variation of Young's modulus and other elastic constants with T [9]. Study of Young's modulus in a polycrystalline wire specimen by the sonic technique is difficult and expensive. A major problem is that to maintain a constant and uniform temperature, the specimen has to be thin, a feature which makes it unsuitable for the sonic tests. We have therefore carried out arranged conventional stress-strain measurements, using a 1-mm-dia x 56 mm wire for which a uniaxial stress can be assumed. The specimen is surrounded by water, the temperature of which can be changed at a controlled rate. A fixed strain below 0.4%, which is well within the

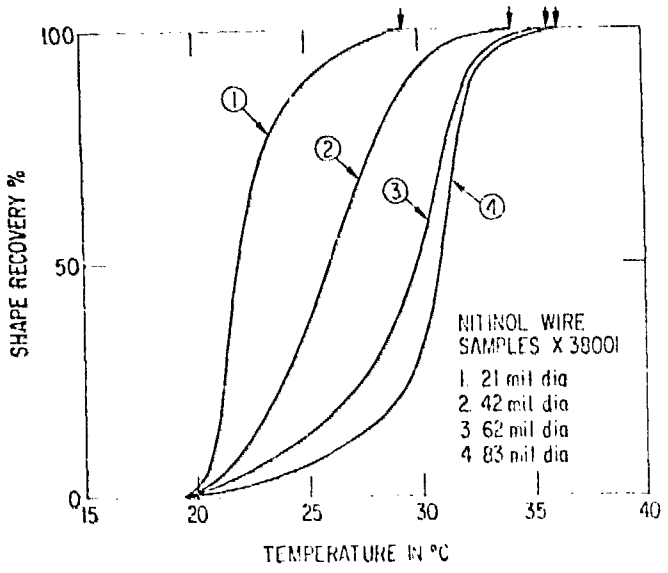

Fig. 4. Fractional shape recovery versus temperature.

elastic state of the Nitinol material, is applied to the specimen, and the variation of σ with T is recorded. At fixed $\varepsilon \leq 0.4\%$, $\Delta\sigma$ is related to ΔE by

$$\Delta E = \frac{1}{\varepsilon} \Delta\sigma \ . \tag{11a}$$

Figure 5 shows the test results for $\varepsilon \approx 0$, 0.18, and 0.36%. Curve (3), corresponding to $\varepsilon \approx 0$, indicates the change $\Delta\sigma$ which is due to the constraint force of the machine jaws (this force prevents the specimen's expansion as T increases). Taking this constraint force into account, the test results give

$$\left\langle \frac{\Delta E}{E} \right\rangle = 4 \ , \tag{11b}$$

where E, defined for 0.05% deviation from linearity, is Young's modulus for the specimen with a martensitic structure. Figure 5 shows that ΔE begins to appear at $T_C \approx 25\text{-}41°C$.

(b) Resistivity change. The athermal resistivity change $\Delta\rho$ that accompanies the change in T during the M$\rightleftarrows$P transformation have been investigated for many SM materials [10]. A plot of typical data for a Nitinol specimen, shown in Fig. 6, exhibits an anomalous shape which has not been adequately explained to date. This anomaly has been shown to be nearly independent of the heating and cooling rates [10]. Nevertheless, our studies indicate that these rates, as well as the specimen structural conditions (internal stress, impurities, etc.) do influence, to some degree, the ρ-T curves. Therefore, to analyze the relationship between the M$\rightleftarrows$P reaction and the ρ-T curves, we have conducted a series of isothermal tests; the results for one well-annealed thin-

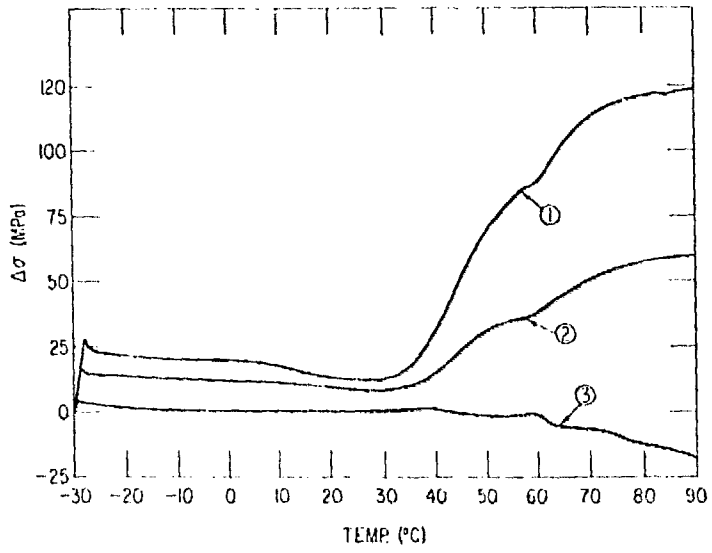

Fig. 5. Transient plots of $\Delta\sigma$ vs T for a Nitinol wir wire specimen under sub-elastic strains $\varepsilon \sim 0$ (curve 1), 0.18 (curve 2), and 0.36% (curve 3).

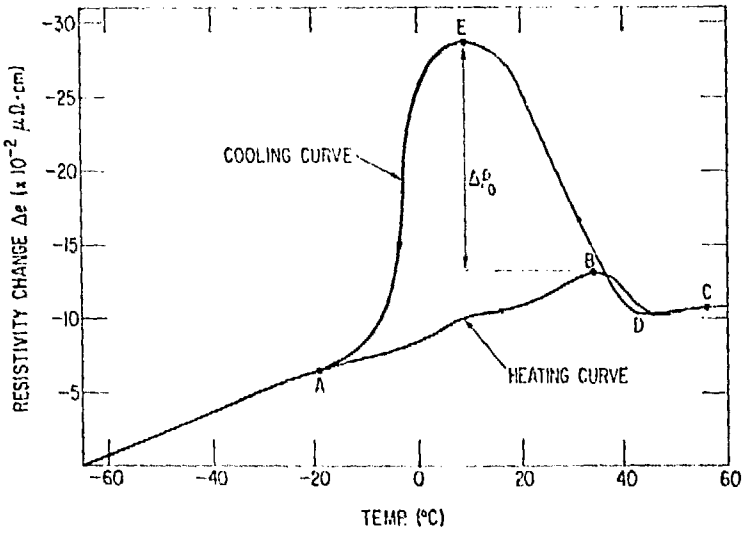

Fig. 6. Athermal resistivity change in a Nitinol wire specimen under zero stress, heated and cooled in a water reservoir at an average rate of 1°C/min.

wire Nitinol specimen, under zero stress, are shown in Fig. 7. Similar tests will be conducted in the future on other Nitinol alloys and on specimens under various combinations of temperature and stress. We note that for either below or above the transition temperature range defined by $T_o^{\pm} = T_o \pm \Delta T_o$, the variation in the resistivity ρ is dominantly ohmic in nature, and its value, denoted by ρ_T, is found as

$$\Delta\rho_T = a\Delta T \qquad (12a)$$

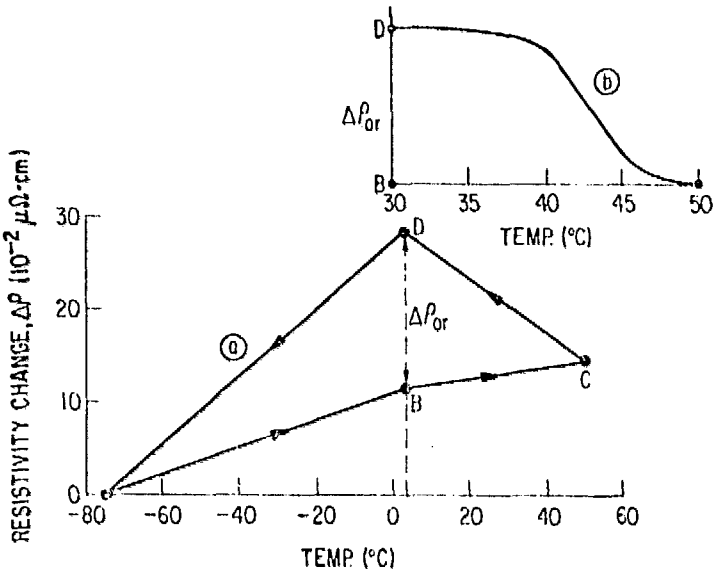

Fig. 7. (a) Hysteresis loop generated by successive isothermal resistivity measurements at temperatures of -75, 4, T_H = 50, 4, and -75°C; (b) the variation of the height of the loop, $\Delta\rho_{or}$, with temperature.

where

$$a = 0.156\ \mu\Omega\cdot cm \quad \text{for} \quad T < T_o^- \qquad (\gamma'\text{-structure}),$$

$$\sim 0.1\ \mu\Omega\cdot cm \quad \text{for} \quad T > T_o^+ \qquad (\beta\text{-structure}). \qquad (12b)$$

However, between T_o^- and T_o^+ the ρ value depends on the structural condition, i.e., the relative proportions of β and γ', internal stresses, impurities, etc. In any case, the isothermal ρ data form a hysteresis loop if a sequence of measurements is made at temperatures T_L', T_L, and T_H, where $T_L' \lesssim M_s$ (say -75°C for our specimen) and $T_L < T_o^-$ (say 4°C). This loop, which is shown schematically by the line ABCDA in Fig. 7a, is reproducible, although it can be changed to the loop ACDA by measuring ρ over the temperature cycle T_L'-T_H-T_L-T_L'. We observe that if we vary T_H between T_o^- and T_o^+, the points A and B do not change. However, as T_H goes toward T_o^-, D approaches B; when T_H reaches T_o^-, the loop reduces to the line AB. The variation in the height of the loop, BD, with respect to T_H is seen in Fig. 7b. This height goes toward zero as the temperature T_L approaches T_H, or T_L'. So by constructing a series of loops for various T_H and T_L values, we can build up the same loop that was obtained by the athermal ρ-T experiment in Fig. 6. In doing this for our specimen, we find T_o = 35°C and $\Delta T_o = \pm 15$°C. Also from the test data we find that ρ_H and ρ_C, which denote the resistivity in heating and cooling, respectively, are functions $(T_H - T_o^+)$ and $(T_L - T_o^-)$. In fact we find phenomenologically, the resistivity changes during the M→P and P→M reactions, respectively, as

$$\Delta\rho_H = \Delta\rho_{or}\left[1 - e^{-K(T-T_o^-)} + e^{K'(T_o^+-T)}\,\theta(T - T_o^+)\right] 0(T - T_o^-)\,0(T_o^+ - T) \qquad (13a)$$

$$\Delta\rho_C = \Delta\rho_{or}\left[e^{-K(T_o^+ - T)} + e^{-K''(T_o^- - T)}\,0(T_o^- - T)\right]\,0(T - T_o^-)\,0(T_o^+ - T)\ . \tag{13b}$$

Here $\Delta\rho_{or}$ is the maximum change in specimen resistivity during the reaction; the coefficients K, K', and K" are constants which depend on the material structural conditions and the heat-transfer coefficient between the specimen and the cooling or heating medium; T_{II} is the temperature at which the heating is reversed to cooling; and the 0 functions guarantee the contribution of each term to a specific temperature range. Thus, $0(T - T_o) = 1$ for $T > T_o$, 0 for $T < T_o$, and so on. In Fig. 6 the AB portion of the heating curve OABD, and the EA portion of the cooling curve CDEAO, are due to the terms containing K' and K", respectively. Making use of Eqs. (12a) to (13b), the difference $\Delta\rho_o$ between the peaks of the cooling and heating curves, in Fig. 6, can be approximated as

$$\Delta\rho_o \simeq a(T_E - T_B) + \Delta\rho_{or}\left[1 + e^{-K''(T_B - T_o^-)} - e^{-K'(T_o^+ - T_E)}\right]\ , \tag{14}$$

From Fig. 6 we find $T_E = 10°C$ and $T_B = 35°C$, and from the isothermal data $\Delta\rho_{or} \simeq 17.5\ \mu\Omega\cdot cm$; combining these data with those in Eqs. (12) to (14), we obtain $\Delta\rho_o \simeq 14\ \mu\Omega\cdot cm$, which agrees with the value obtained from Fig. 6.

(c) Thermoelectric power in the M-P reaction. The measurement of the thermal emf generated at interfaces between the M and P phases is rather difficult because of the interference from the thermoelectric power generation at the specimen junctions. To eliminate this effect, we first measured the thermoelectric power of Nitinol relative to metals such as Cu, Ni, Ag, and Au. We found that the conventional polarity of Nitinol relative to these materials depends on whether the Nitinol is in the M or the P phase. For example, relative to the absolute thermoelectric power values for Cu and Ni in $\mu V/°C$, we found [11]

P-phase	Cu	Ni	M-phase
+11.7	+1.5	-16.8	-45.3

Use of a long (50-cm) specimen with copper leads minimized the junction effects satisfactorily. The specimen was curved so that any portion of it could be immersed in the water reservoir. The specimen junctions were kept at about 0°C by covering them with several layers of frozen insulating materials. The specimen was cooled in a CR to produce the M structure; a portion or the entire specimen was then rapidly immersed in an HR to produce P phase. We found that during the M→P transition an emf of 0.1 to 0.12 mV was generated. This emf will remain constant as long as the M and P zones in the specimen are maintained. The M-phase is negatively charged relative to the P-phase, so that in conventional terms the P-phase is the positive pole. In a wire specimen in which a P zone is sandwiched between two M zones, as in Fig. 8, the sign of the emf depends on the lengths of the M zones.

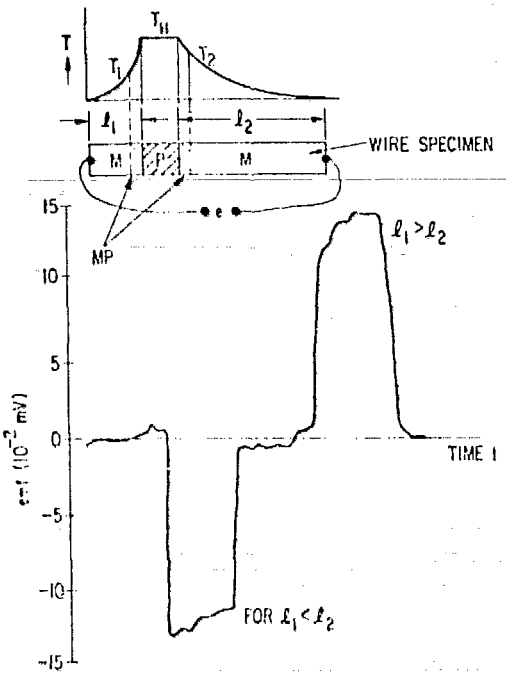

Fig. 8. The net thermal emf e generated in a long Nitinol wire specimen with a P-phase region sandwiched between two M-phase regions. PM indicates the two M-P interfacial zones.

This may be explained as follows: Assume the specimen terminal junctions are kept at 0°C, and the P zone is at temperature T_H, so that thermal gradients are present in the M zones (with lengths ℓ_1 and ℓ_2. Then the thermoelectric fields on the two sides of the P zone can, in general, be written as

$$E_{MP} = Q_{MP}\left(\frac{dT}{d\ell}\right)_{\ell} \quad . \tag{15a}$$

Here $dT/d\ell$ is the thermal gradient from 0 to T_H (in °K) along the wire portion with length ℓ; Q_{MP} is the interfacial thermopow · (in V/°K) generated by the thermal diffusion and phonon drag between the M zone and the P zone. Note that in the present case, Q_{MP} appears only because of the M>P reaction; i.e., $Q_{MP} = 0$ for $T_H \leq T_o^-$, but Q_{MP} is a constant as long as the M and P zones can be maintained and $T_H \geq T_o^+$. Hence,

$$Q_{MP} = Qe^{k(T-T_o^+)}0(T_o^+-T)0(T - T_o^-) \quad , \tag{15b}$$

where k is a constant and Q depends on the free electron path and area of the Fermi surface associated with the P-M admixture in the interfacial zone. Now if $\ell_1 \neq \ell_2$, the M-P interfacial zones in Fig. 8 have different thicknesses and are under different temperature gradients. Thus, according to Eqs. (15a) and (15b), the net emf across the specimen can be written as

$$E = Q_{MP}[T_1 - T_2] \quad , \tag{15c}$$

where T_1 and T_2 are the temperatures at the two M-P interfacial zones, as shown in Fig. 8. The sign of E depends on the magnitudes of the thermal gradients along the ℓ_1 and ℓ_2 portions; E vanishes for $\ell_1 = \ell_2$, in agreement with the test result. This interfacial emf does not vary

with T_H and T_L. Experimental results, a sample of which is shown in Fig. 8, lead to $Q_{MP} \simeq -0.12$ mV, in agreement with the thermoelectric data given above for the P and M phases. The negative sign of Q_{MP} agrees with the general expectation that the current flows from the hot section (P-phase) to the cold one (M-phase).

IV. Concluding Remarks

It is clear that the martensitic transformation in SM alloys generates many changes in the metal properties which are nearly reversible as soon as the reverse reaction occurs. Two distinct martensitic transformations are involved in the process. The first, $\gamma' \rightarrow \beta$, is a first-order transformation in many respects. The volume change due to this transformation is apparently very small ($\sim$0.1%) in Nitinol materials. The anomalous shape of the specific-heat or resistivity change, associated with the first-order λ-type transformation, is very similar to that in ferromagnetic materials. However, unlike the ferromagnetic transformation, the present transition preserves the ordering state. The shallow minima in the ΔE variations in Fig. 5, and the broad peaks in the ρ curves in Fig. 6, is partly due to the second-order phase change caused by straining and partly due to the fact that the specimen is polycrystalline and the transition temperature exhibits a spread of $2\Delta T_o$.

The unusual change in Young's elastic modulus with temperature is readily understandable. As a well-annealed alloy with the γ' structure, Nitinol is extremely pliable, whereas the same material in the β phase is highly elastic. The mechanical properties of the M and P structures are consistent with the γ' and β' electronic states.

Note that while the increase in $\Delta E/E$ is due to the $\gamma' \rightarrow \beta$ transition, the nonzero value of $W_o - W_i = \Delta W$ in the energy-balance equation (1) is due solely to the indirect $\gamma' \rightarrow \beta' \rightarrow \beta$ reaction which takes place by "reshuffling" of the highly unstable γ' variants at a temperature $T_H > T_C$ and under an applied stress. It would be interesting to find out whether the coefficient α in Eq. (1), which leads to $\Delta W \neq 0$, can be increased from its present value of 0.14 by changing the alloy composition, impurity content, etc. The variation of T_C with the grain size and density, Eq. 10, needs future investigation.

The isothermal resistivity measurement provides a fairly accurate method of study of the M-P transition in terms of T, σ, and material parameters. It reveals the source of the anomaly in the ρ-T curves. From the test data leading to Eqs. (12a) to (13b), we find that the existence of the transition range ΔT_o, even with residual P phase below T_o^-, cannot be responsible for the ρ-T anomaly. One then must explain how at a given $T_L < T_o$ the martensite can have two different ρ values, as shown by points D and B in Fig. 8a. To do this we note that ρ depends on the phonon-electron scattering amplitude (call it A) projected along a given crystal axis that is oriented along the current direction. In a (cubic) P-structure, A is the same for any of the crystal axes. On the other hand, in an M-structure formed by inhomogeneous rapid cooling, internal stresses cause various degrees of lattice distortion (producing a metastable M-structure); this leads to the variation of

A, and "Charge Density Wave" and, in turn, an increase in ρ as shown by point D [12]. However, during a relaxation period which depends on T_L-T_o, the lattice distortion is minimized and some phonon modes are dissipated; thereby a more stable M-structure with lower ρ (shown by point D) is produced. This stabilization process is accelerated exponentially if T_L is lowered. Finally we note that the thermoelectric pulse shown in Fig. 8, arises between the P and stable M phases with a metastable M-P interfacial zone. More detailed information on the resistivity and thermopower will be presented in a separate article.

An important observation is that all these changes (in the M→P interfacial emf, electrical resistivity, and elastic constants) share a common parameter, namely, the Debye temperature Θ, which is a measure of the interaction between the thermal phonons and electronic states of the materials. The variation of Θ during the M→P reaction has already been reported for the (Cu, Au, Zn) shape-memory alloys [13]. Another important parameter seems to be the strong anisotropy factor, C_{44}/C', which appears at the SR critical temperature T_C. This phenomenon suggests that in addition to the phonon-electron interaction, the phonon-lattice interaction should be taken into account. All these points are currently under study as a continuation of the present work. Finally, the effects of stress on the resistivity thermoelectric power, etc. will be reported in a separate paper.

Work supported by the U.S. Department of Energy.

Acknowledgments

The author would like to thank Drs. W. J. Shack and E. Fisher for many useful comments and discussions.

References

[1] Numerous articles have been published on the shape recovery and other features of the martensitic transformation in some shape-memory alloys. However, relatively little has been presented on the Ni-Ti shape-memory alloys since the report of C. M. Jackson, R. J. Wagner, and R. J. Wasilewski: NASA-SR 5110, 1972 (unpublished).

[2] See Ref. 1 and R. H. Eckelmeyer: "Effect of Alloying on the Shape Memory Phenomenon in Nitinol," Tech. Report SAN 74-0418, Sandia Laboratories (March 1975).

[3] A. A. Golestaneh has proposed a systematic investigation of the SRP in "The Shape-Recovery Phenomenon in Shape Memory Alloys, with Particular Reference to the Nitinol Systems," Tech. Report, Argonne National Laboratory (Sept. 1978).

[4] A. A. Golestaneh: to be published.

[5] A. A. Golestaneh: J. Appl. Phys., 49, (1241), 1978.

[6] See, for instance, Jackson et al. (Ref. 1).

[7] Note that the CC equation has only been derived for first-order reactions in the liquid-gas systems. The application of this equation to a system involving stress and strain tensors needs experimental verification, as provided in the present work.

[8] For example, G. Edwards and J. Perkins: *Shape Memory Effects in Alloys*, Ed. by J. Perkins, Plenum, New York (1975), 445.

[9] Variations of the bulk of modulus, elastic constants, and Poisson's ratio in Nitinol systems have been studied by several authors, e.g., N. G. Pace and G. A. Saunders: Phil. Mag., 22 (1970), 73.

[10] F. E. Wang, B. F. DeSavage, W. Buehler, and W. R. Hosler: J. Appl. Phys., 39 (1968) 2166.

[11] A gold junction with special soldering material was used to minimize the junction thermocouple effect.

[12] The anisotropy in the A amplitude plays the same role in forming the resistivity hysteresis loop as the magnetization in the ferromagnetic case. Hence it may be possible to develop a theory for the ρ loop following the approach used for the magnetic hysteresis loop.

[13] See, for instance, N. Nakanishi, Ref. 8, p. 151. The linkage between the Debye temperature and several features of the M↔P transformation in the SM is under study by A. A. Golestaneh.